IOPscience iopscience.iop.org

Home Search Collections Journals About Contact us My IOPscience

Thermodynamics and conformational changes related to binding of eIF4E protein to mRNA 5' cap

This article has been downloaded from IOPscience. Please scroll down to see the full text article.

2005 J. Phys.: Condens. Matter 17 S1483

(http://iopscience.iop.org/0953-8984/17/18/006)

View the table of contents for this issue, or go to the journal homepage for more

Download details:
IP Address: 129.252.86.83
The article was downloaded on 27/05/2010 at 20:41

Please note that terms and conditions apply.

INSTITUTE OF PHYSICS PUBLISHING JOURNAL OF PHYSICS: CONDENSED MATTER

J. Phys.: Condens. Matter **17** (2005) S1483–S1494 doi:10.1088/0953-8984/17/18/006

Thermodynamics and conformational changes related to binding of eIF4E protein to mRNA 5′ cap

Anna Niedzwiecka[1,2,3], **Edward Darzynkiewicz**[2] **and Ryszard Stolarski**[2]

[1] Biological Physics Group, Institute of Physics, Polish Academy of Sciences, 32/46 Lotnikow Avenue, 02-668 Warsaw, Poland
[2] Department of Biophysics, Institute of Experimental Physics, Warsaw University, 93 Zwirki and Wigury Street, 02-089 Warsaw, Poland

E-mail: annan@ifpan.edu.pl

Received 30 September 2004, in final form 25 January 2005
Published 22 April 2005
Online at stacks.iop.org/JPhysCM/17/S1483

Abstract

Molecular bases of biological activity of proteins do not flow naturally from crystal structures. Proteins and ligands in solution are not rigid and undergo conformational changes upon binding. The formation of functional macromolecular complexes is also accompanied by interactions with the environment. Hence, the static structural view needs to be supplemented by thermodynamic and hydrodynamic descriptions.

eIF4E is a regulatory protein, which specifically recognizes the mRNA 5′-terminal cap structure at the initial, rate-limiting step of translation in eukaryotes. Interactions of eIF4E with chemical cap analogues have been studied by means of emission spectroscopy and dynamic light scattering. The thermodynamic parameters have been determined by a van't Hoff analysis of equilibrium association constants. At biological temperatures, binding of the natural caps is both enthalpy- and entropy-driven. Values of heat capacity changes correlate with the free energies of eIF4E-cap binding. Coupling of eIF4E-cap association to intramolecular self-stacking of dinucleotide cap analogues makes the binding entropies less negative. Isothermal enthalpy–entropy compensation at 293 K ($T_c = 399 \pm 24$ K) points to significant fluctuations of the *apo*-protein and its stiffening in the complex. DLS measurements showed that interaction of cap analogues with aggregated eIF4E led to the dissociation of eIF4E to the native, monomeric structure.

(Some figures in this article are in colour only in the electronic version)

1. Introduction

All eukaryotic messenger ribonucleic acids (mRNAs) and small nuclear ribonucleic acids (snRNAs) that are transcribed in the nucleus possess a so-called '5′ cap' (m^7GpppN) in

[3] Author to whom any correspondence should be addressed.

 © 2005 IOP Publishing Ltd Printed in the UK

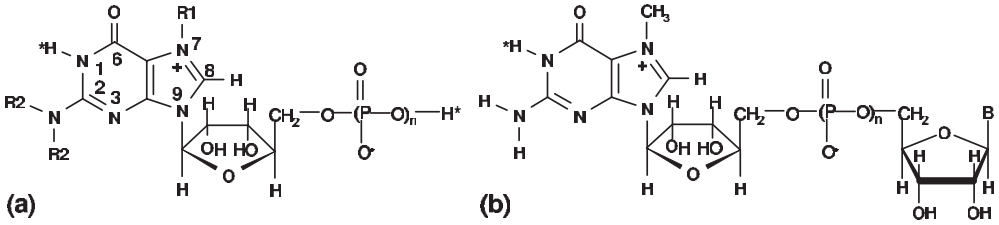

Cap analogue	R1	R2	n	Cap analogue	n	B
m^7GMP	CH_3	H	1	m^7GpppG	3	G
m^7GDP	CH_3	H	2	m^7GpppC	3	C
m^7GTP	CH_3	H	3	m^7Gpppm^{7}G	3	m^7G
bz^7GTP	CH_2-Φ	H	3	m^7GppppG	4	G
p-Cl-bz^7GTP	CH_2-Φ-Cl	H	3	m^7Gppppm^{7}G	4	m^7G
$m_3^{2,2,7}$GTP	CH_3	CH_3	3			

Scheme 1. Structures of cap analogues used in the studies; Φ denotes the phenyl ring; protons that partially dissociate at pH 7.2 are marked with an asterisk ($pK_a^{N(1)-H} \sim 7.24$–7.54, depending on R2 and *n* [39]; $pK_a^{\text{phosph}} \sim 6.1$–$6.5$, depending on *n* [40]). According to recent results, the positive charge at the five-member ring of the 7-methylguanosine moiety is localized at N^7 [41].

which 7-methylguanosine is linked by the 5′-5′-triphosphate bridge to the first nucleoside [1] (scheme 1). The 5′ cap structure is necessary for optimal mRNA translation [1], RNA nuclear export [2], and splicing of mRNA precursors [2], and it affects the mRNA stability [3]. After nuclear export to the cytosol, the cap of snRNAs is further methylated at the amino group of the guanosine moiety, forming a trimethylguanosine cap, $m_3^{2,2,7}$GpppN [4]. This structure is responsible for import of the snRNA-protein spliceosomal complexes (snRNPs) back into the nucleus [5], where snRNPs take part in pre-mRNA splicing [6].

During initiation of translation, the correct starting site on mRNA is identified and binding of the ribosome occurs. Regular translation initiation in eukaryotes is mainly 5′ cap-dependent. The monomethylguanosine cap function in translation initiation is mediated by the eukaryotic initiation factor 4E (eIF4E) [7], which is the smallest subunit (25 kDa) of the heterotrimeric eIF4F preinitiation complex containing also the scaffolding eIF4G protein and the eIF4A factor which is an mRNA helicase [8] (scheme 2). Interaction between eIF4E and eIF4G is regulated by 4E-binding proteins (4E-BPs) [8], which block the eIF4G-binding site on eIF4E. Accessibility of eIF4E for formation of eIF4F is supposed to regulate the overall efficiency of ribosome recruitment [8]. Biological activity of eIF4E is also regulated by its phosphorylation at Ser209 in response to treatment of cells with growth factors, hormones, and mitogens [9]. Phosphorylation decreases the affinity of eIF4E for the mRNA 5′ cap [10], but its biological function is still unclear. The three-dimensional structures of mammalian eIF4E bound to m^7GDP [11], m^7GpppG [12], m^7GTP and m^7GpppA [13] were solved by crystallography. The cap analogue is located in a narrow cap-binding slot on the concave surface of eIF4E

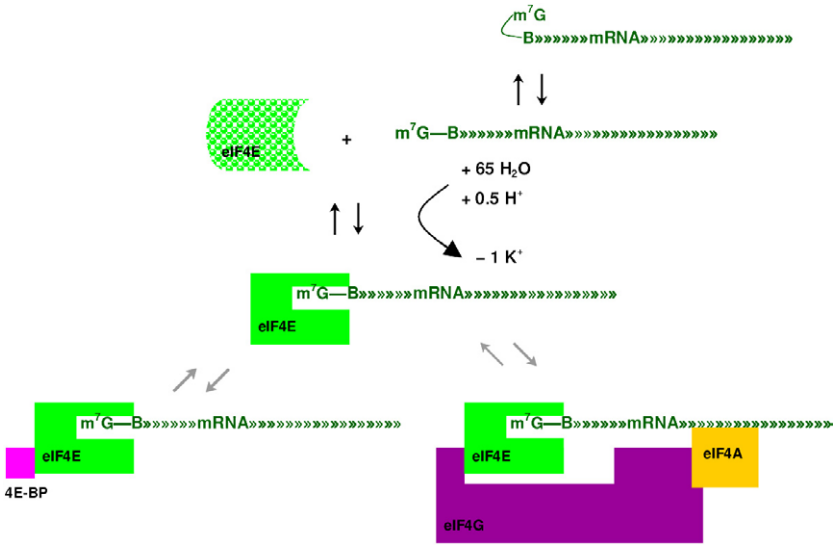

Scheme 2. The processes involved in the first step of initiation of translation. Association of eIF4E with the capped mRNA is thermodynamically coupled to the stacking/unstacking equilibrium of 7-methylguanosine (m^7G) with the first transcribed nucleoside (B), the uptake of about 65 water molecules, the partial protonation of 7-methylguanine moiety at $N(1)$ (see scheme 1), and the release of one monovalent cation (K^+), and is accompanied by a conformational change of the protein. The eIF4E–mRNA complex can further form the active preinitiation complex with the scaffolding factor eIF4G and the RNA helicase eIF4A (bottom, right), unless it is inhibited by association with the 4E-binding protein (4E-BP, bottom, left).

(figure 1). The cap-eIF4E binding is an electrostatically-steered, two-step process [12, 14]. It is accompanied by (scheme 2) internal rearrangement of the encounter protein–ligand complex [14] and solvent effects, such as the uptake of about 65 water molecules, release of one monovalent cation, and partial protonation at $N(1)$ of the 7-methylguanine moiety of the cap [12, 15] (scheme 1). The latter process ensures binding of the cap in the cationic form (figure 1(c)), since the unbound cap molecules occur at physiological pH in a roughly equimolar amount of the cationic and zwitterionic forms.

eIF4E participates also in nucleocytoplasmic transport of growth regulatory mRNA [16] and is involved in splicing and 3′ mRNA processing [17]. All these additional functions of eIF4E appear to be dependent on its intrinsic ability to recognize the mRNA 5′ cap. Thus, this single biochemical activity of eIF4E is versatile enough to play roles in divergent processes in different cellular compartments during gene expression.

While transcription is responsible for the coarse control of gene expression, translation provides a means for fine regulation. It enables a spatial control of protein synthesis, which plays a key role during early development, underlies processes of learning and memory encoding [18], and is an important factor in human cancer [19]. In particular, the activity of eIF4E plays a pivotal role in translational control of gene expression. It is frequently related to disorder of cellular proliferation, growth and differentiation. Immunological detection of eIF4E was even reported as a useful diagnostic tool to identify malignant cells for removal during surgery of head and neck cancer [20]. On the other hand, enhanced eIF4E activity is necessary for human T lymphocytes to progress from the resting state to proliferation and to attain immune competency [21]. Hence, thermodynamic and conformational investigations leading to a biophysical description of the molecular mechanism of specific recognition of

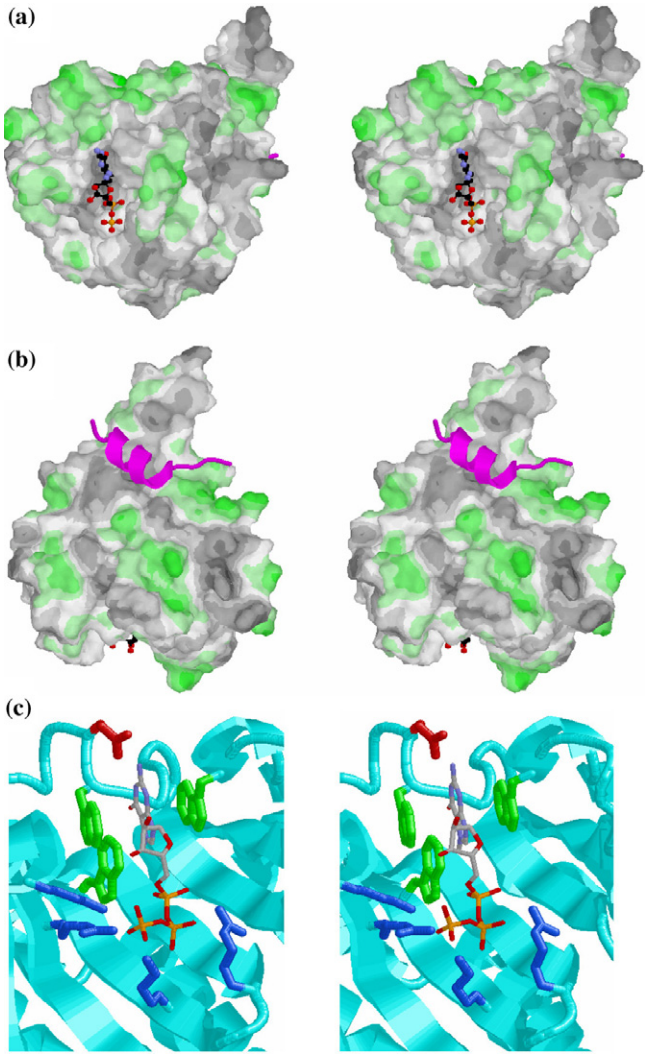

Figure 1. eIF4E (28-217) in the complex with the cap analogue (m^7GDP) and the 4E-BP1 translation factor [35] (PDB #: 1EJ4) showing grey colour-coded hydrophobic surface areas and lighter grey (green) colour-coded polar or charged areas. The cap analogue is drawn as an atomic stick figure. The helical fragment of 4E-BP1 is represented as a (magenta) ribbon. (a) Stereodrawing showing the solvent-accessible concave cap-binding surface of eIF4E. (b) Stereodrawing showing the solvent-accessible convex dorsal surface of eIF4E with the 4E-BPs/eIF4G-binding site. (c) Stereodrawing showing stabilization of m^7GTP (stick representation) inside the eIF4E cap-binding slot (PDB #: 1L8B): the 7-methylguanine cation sandwich stacks in between two tryptophan indole rings (green), and forms three Watson–Crick-like hydrogen bonds involving O^6, $N(1)$ and N^2 of the cap (see scheme 1) with the backbone NH of tryptophan and the carboxylate of glutamic acid (red); negatively charged phosphate groups of the cap interact via salt bridges and direct or water-mediated hydrogen bonds with positively charged (blue) amino acid side chains.

the mRNA 5′ cap structure by eIF4E are of primary importance, especially in the face of the complexity of the binding event (scheme 2). Taking into account that salt bridges, cation-π stacking, and hydrogen bonds play a dominant role in mRNA 5′cap–eIF4E binding [11, 12, 22],

this molecular system is significantly distinct from the hydrophobic systems which are usually a focus of thermodynamic studies. The results discussed herein show that thermodynamic and hydrodynamic studies allow for explanation of some fundamental biological properties of the eIF4E protein.

2. Materials and methods

Chemical syntheses of cap analogues (scheme 1) were performed as described previously [23]. Expression and purification of murine eIF4E (residues 28-217 and residues 33-217) were done without contact with the cap [12, 24]. All other chemicals were of analytical grade, purchased from Sigma-Aldrich, Merck, Carl Roth (Germany) or Fluka (USA).

Fluorescence measurements. Absorption and fluorescence spectra were recorded on Lambda 20 UV/VIS and LS-50B instruments (Perkin-Elmer Co., Norwalk, CT, USA), in a quartz semi-micro cuvette (Hellma, Germany) with a magnetic stirrer and optical lengths of 4 and 10 mm for absorption and emission, respectively. Titration experiments leading to the determination of the temperature-dependent association constants (K_{as}) for eIF4E (28-217) and m^7GMP, m^7GDP, m^7GTP, bz^7GTP, *p*-Cl-bz^7GTP, $m_3{}^{2,2,7}$GTP, m^7GpppG, m^7GpppC, m^7Gppppm^{7}G, were performed in 50 mM HEPES/KOH pH 7.20, 100 mM KCl, 1 mM DTT and 0.5 mM EDTA, and analysed as described in detail previously [12, 25]. The temperature was controlled to ±0.2 K inside the cuvette with a thermocouple.

Thermodynamics. The fluorimetrically measured association constant (K_{as}) at a given temperature (T) is directly related to the standard molar Gibbs free energy (ΔG°) of association:

$$\Delta G^\circ = -RT \ln K_{as}, \tag{1}$$

where the binding constants (K_{as}) were used for asymmetrical cap analogues and the microscopic binding constants ($K_{as}^{micro} = 0.5 \cdot K_{as}$) for symmetrical cap analogues due to entropic effects (the index '°' refers to the pseudostandard state at concentrations of 1 mol l^{-1}, i.e. unit molarity; R is the gas constant).

In an isothermic–isobaric process, ΔG° is expressed in terms of the standard molar enthalpy (ΔH°) and entropy (ΔS°) of association:

$$\Delta G^\circ = \Delta H^\circ - T\Delta S^\circ. \tag{2}$$

The temperature dependence of K_{as} was analysed according to the van't Hoff isobaric equation:

$$\ln K_{as} = \frac{\Delta S^\circ}{R} - \frac{\Delta H^\circ}{RT}. \tag{3}$$

If the system did not reveal a non-zero standard molar heat capacity change (ΔC_p°), the enthalpy and entropy changes were independent from temperature and were directly fitted as constant values.

If ΔC_p° differed from zero and was independent from temperature, then the enthalpy and entropy changes were expressed as

$$\Delta S^\circ = \Delta C_p^\circ \ln\left(\frac{T}{T_S}\right) \tag{4}$$

$$\Delta H^\circ = \Delta C_p^\circ (T - T_H) \tag{5}$$

and the van't Hoff plot, i.e. the plot of $\ln K_{as}$ versus $1/T$, became non-linear in respect to the reciprocal of the absolute temperature (abscissa variable) [26]:

$$\ln K_{as} = \frac{\Delta C_p^\circ}{R}\left[\frac{T_H}{T} - \ln\left(\frac{T_S}{T}\right) - 1\right]. \tag{6}$$

In this case, the molar heat capacity change (ΔC_p°) and the characteristic temperatures (T_S where $\Delta S^\circ = 0$, and T_H where $\Delta H^\circ = 0$) were obtained as free parameters of the fitting.

Intrinsic values of the thermodynamic parameters for interactions of eIF4E with the unstacked dinucleotide cap analogues (scheme 2) were calculated according to the equations describing mandatory coupling between binding and self-stacking [27, 28].

Data analysis was carried out on the basis of the runs test and the P-value [29]. The goodness of fits of the binding isotherms (R^2) was $\geqslant$0.999. Discrimination between the two forms of the van't Hoff equation (equations (3) and (6)) was based on Snedecor's F-test [29], with the significance level of $P(\nu_1, \nu_2) < 0.05$. Errors (one standard deviation) were calculated according to the propagation rules [30]. Isothermal enthalpy–entropy compensation was analysed including uncertainties of both ΔH° and ΔS°. Regressions were performed by means of the least-squares method, using PRISM 3.02 (GraphPad Software Inc., USA) or ORIGIN 6.0 (Microcal Software Inc., USA).

Dynamic light scattering. The DLS measurements were run on a DynaPro-801 Molecular Size Detector (Protein Solutions Inc., USA) for eIF4E (33-217) at a concentration of 1 mg ml^{-1}, in the absence and in the presence of 50-fold excess of m^{7}GTP, p-Cl-bz^{7}GTP, m$_3^{2,2,7}$GTP, m^{7}GpppG, m^{7}Gpppm^{7}G, m^{7}GppppG, or m^{7}Gppppm^{7}G, at 293 K, in 50 mM HEPES/KOH pH 7.20, 100 mM KCl, 1 mM DTT and 0.5 mM EDTA. Molecular weight calculations were performed by means of a logarithmic function provided by the manufacturer of the DLS equipment.

For approximately globular proteins, the hydrodynamic radius (R_h) is related to the diffusion coefficient (D). Fluctuations in the intensity of light scattered by a small volume of a solution are described by an autocorrelation function ($g_1(t)$). For small monodispersed particles and homogeneous spheres the normalized autocorrelation function of scattered electric field is [31]

$$g_1(t) = \mathrm{e}^{-D\vec{Q}^2 t}, \tag{7}$$

where $\vec{Q}$ is the scattering vector, and t is the time interval for displacement of the scattering particle. D is related to the reciprocal of the characteristic decay time (Γ):

$$\Gamma = D\vec{Q}^2. \tag{8}$$

For polydispersed systems with different Γ values,

$$g_1(t) = \sum_i a_i \mathrm{e}^{-\Gamma t}, \tag{9}$$

where the a_i are amplitudes, proportional to the molecular weight and concentration of species. In terms of cumulant analysis [32], the above equation can be developed into

$$\ln g_1(t) = -\bar{\Gamma} t + \mu_2 t^2 + \cdots, \tag{10}$$

where $\bar{\Gamma}$ is the first cumulant related to the average decay rate and μ_2 is the second cumulant (normalized variance of the distribution) related to the polydispersity index (PDI):

$$\mathrm{PDI} = \frac{\mu_2}{\bar{\Gamma}^2}. \tag{11}$$

An inverse Laplace transform generates the decay rates from which the diffusion coefficients and then the particle sizes can be determined using the Stokes–Einstein equation:

$$D = \frac{k_\mathrm{B} T}{6\pi\eta R_\mathrm{h}}. \tag{12}$$

Visualization of the solvent accessible surface of eIF4E in the complex with cap and 4E-BP1 was done by means of Protein Explorer [33].

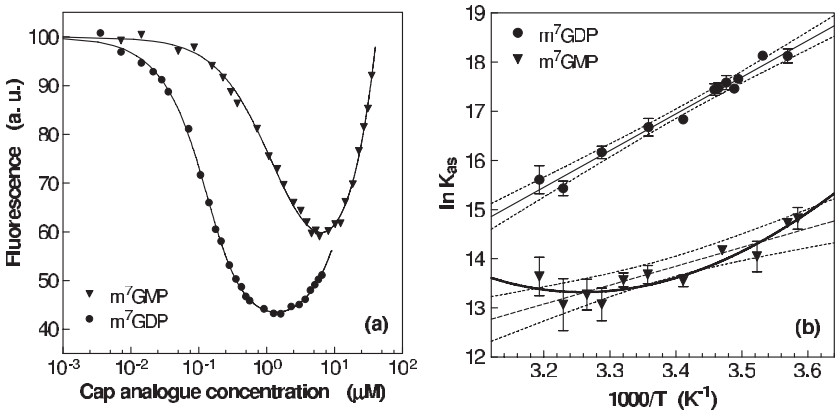

Figure 2. (a) Isotherms of binding (293 K) of m^7GMP and m^7GDP to eIF4E (28-217) at 0.1 μM, and the corresponding fitting residuals. An increasing fluorescence signal at higher cap concentrations originates from emission of the free cap in solution. (b) van't Hoff isobars describing interactions of eIF4E with m^7GMP and m^7GDP. The non-linear fit in respect to $1/T$ (▬) for m7GMP is better than the linear fit (——) at the significance level of 0.027.

3. Results and discussion

3.1. Thermodynamics of eIF4E–mRNA 5′ cap binding

The thermodynamic parameters describing the interaction of eIF4E (28-217) with a series of synthetic cap analogues have been determined from the van't Hoff method, on the basis of equilibrium association constants obtained from fluorescence titrations (figure 2). Standard molar enthalpy changes (ΔH°) and entropy changes (ΔS°) at 293 K are collected in table 1. Association of eIF4E to mRNA 5′ cap at 293 K has been found generally to be enthalpy-driven, and entropy-opposed or -driven, depending on the cap analogue. The enthalpy change plays a more pronounced role for binding of the analogues with longer negatively charged phosphate chains, which is entropy-opposed. The binding entropy is more conducive to association of the analogues possessing either more or larger substituents at the guanine moiety.

For the analogues of moderate affinity to eIF4E, the thermodynamic parameters that are linked to the non-linearity of the van't Hoff plot (equation (6)) have been detected, i.e., standard heat capacity change under constant pressure (ΔC_p°), and the critical temperatures T_H and T_S where $\Delta H^\circ = 0$ and $\Delta S^\circ = 0$, respectively (table 1). The large ΔC_p° values are surprisingly positive, from +1.66 up to +5.12 kJ mol^{-1} K^{-1}, and T_H is higher than T_S. The positive heat capacity changes were confirmed independently by direct calorimetric measurements of eIF4E interaction with m^7GpppG, for which $\Delta C_{p\,\mathrm{cal}}^\circ = +1.94 \pm 0.06$ kJ mol^{-1} K^{-1} [15]. The positive ΔC_p° values are mainly related to the increase of the water-exposed hydrophobic protein surface [26, 34]. In the case of small ligand binding to proteins, such large ΔC_p° values render conformational changes of the protein that influence the water accessibility of the protein surface. eIF4E possesses a widespread hydrophobic surface at the opposite side to the cap-binding slot, near the partially unstructured N-terminal tail of eIF4E (figure 1). This region is responsible for interactions with other translation factors, i.e., eIF4G and 4E-BPs [35].

The less positive ΔC_p° values for the cap analogues of higher affinity suggest that there is an increasing negative contribution coming from protein stiffening in the most tightly bound complexes [34]. Thus, both the positive values of the heat capacity changes and their dependence on the affinity of the cap analogue to eIF4E are evidence of significant conformational transition of eIF4E upon cap binding.

Table 1. Standard molar enthalpy changes (ΔH°) at 293 K, entropy changes (ΔS°) at 293 K, Gibbs free energy changes (ΔG°) at 293 K, heat capacity changes under constant pressure (ΔC_p°), and critical temperatures T_H (where $\Delta H^\circ = 0$) and T_S ($\Delta S^\circ = 0$) for binding of eIF4E to mRNA 5′ cap analogues. Corresponding thermodynamic parameters (indexed '0') for intrinsic binding of eIF4E to the unstacked from of dinucleotide cap analogues[a].

Cap analogue	ΔH° (kJ mol^{-1})	ΔS° (J mol^{-1} K^{-1})	ΔG° (kJ mol^{-1})	ΔC_p° (kJ mol^{-1} K^{-1})	T_H (K)	T_S (K)
m^7Gp	-36.0 ± 7.9	-9.3 ± 3.4	-33.15 ± 0.20	$+2.62 \pm 0.97$	306.9 ± 4.8	294.20 ± 1.68
m^7Gpp	-61.9 ± 2.9	-69.8 ± 10.5	-41.031 ± 0.179	n. d.	n. d.	n. d.
m^7Gppp	-74.3 ± 3.6	-98.7 ± 12.1	-45.109 ± 0.090	n. d.	n. d.	n. d.
bz^7Gppp	-56.5 ± 3.8	-52.7 ± 13.0	-40.669 ± 0.060	n. d.	n. d.	n. d.
p-Cl-bz^7Gppp	-38.5 ± 4.6	$+16.7 \pm 15.5$	-42.94 ± 0.21	n. d.	n. d.	n. d.
$m_3{}^{2,2,7}$Gppp	-16.6 ± 2.5	$+40.3 \pm 12.7$	-28.94 ± 1.36	$+5.12 \pm 0.48$	296.41 ± 0.43	290.86 ± 0.69
m^7Gppppm^7G[b]	-81 ± 54	-136 ± 88	-41.377 ± 0.146	$+1.66 \pm 0.57$	342.0 ± 16.0	318.0 ± 7.8
m^7GpppG	-65 ± 31	-91 ± 58	-38.555 ± 0.152	$+1.92 \pm 0.93$	327.1 ± 15.2	307.4 ± 6.0
m^7GpppC	-50 ± 28	-45 ± 29	-36.42 ± 0.40	$+2.96 \pm 1.25$	310.0 ± 6.2	297.6 ± 2.1
	ΔH_0°	ΔS_0°				
m^7Gppppm^7G[b]	-85 ± 54	-147 ± 88				
m^7GpppG	-75 ± 31	-122 ± 58				
m^7GpppC	-52 ± 28	-50 ± 29				

[a] Data from [12, 15, 28].
[b] The microscopic association constant ($K_{as}^{micro} = 0.5K_{as}$) has been taken into account.

Binding of eIF4E to the mRNA 5′ terminus is directly coupled with intramolecular self-stacking, since only the unstacked form of the dinucleotide cap is capable of forming the complex with eIF4E (scheme 2, figure 1). Self-stacking of the cap provides for additional enthalpic and entropic contributions, and for an apparent molar heat capacity change, resulting from an induced shift in the conformational equilibrium of the ligand upon binding to the protein [27]. The coupling reduces the negative values of the intrinsic enthalpy and entropy changes (ΔH_0°, ΔS_0°) to a substantial extent, leading to the apparently less negative values of the observed ΔH° and ΔS° (table 1). The intrinsic binding free energies (ΔG_0°), the heat capacity changes (ΔC_{p0}°), and the characteristic temperatures (T_{S0}, T_{H0}) for the unstacked cap structures are negligibly changed in comparison with the observed values (constant within SD) [28].

The enthalpic and entropic contributions to the Gibbs free energies of eIF4E-cap binding at 293 K are highly correlated (table 1), with the coefficient $r^2 = 0.975$, and give the slope related to the enthalpy–entropy compensation temperature $T_c = 399 \pm 24$ K. The result is the same for the data sets of either the intrinsic (ΔH_0°, ΔS_0°) or the observed (ΔH°, ΔS°) parameters. This means that the general thermodynamic property of recognition of the mRNA 5′ cap by eIF4E is insensitive to self-stacking of the cap. Several critical opinions regarding isothermal enthalpy–entropy compensation within congener series have been published [36, 37]. However, as we showed recently [28], the series of cap analogues satisfies all criteria for the non-trivial, statistically important enthalpy–entropy compensation which reflects some additional, extrathermodynamic information about the macromolecular system, for example about the distribution of energy levels available to the system and the perturbation of this distribution caused by protein–ligand interactions [37]. The compensation temperature, T_c, is related to the difference in conformational stability of the system in the unperturbed and the perturbed states. A difference between the compensation temperature and the harmonic mean experimental temperature can be a measure of the fluctuations of the unperturbed system, which are modulated by the perturbation. The T_c value shows that the energy of the state of eIF4E which binds to the cap structure lies below the mean energy of the *apo*-protein by 9.66 ± 1.7 kJ mol^{-1}. Such a large value suggests that *apo*-eIF4E is a highly fluctuating protein and the specific cap binding causes significant stiffening of the global protein structure.

3.2. Deaggregation of eIF4E induced by mRNA 5′ cap binding

To check whether the hydrophobic dorsal surface of eIF4E undergoes conformational changes caused by interaction within the spatially distant cap-binding slot, hydrodynamic measurements of the aggregation of eIF4E were performed by means of dynamic light scattering (DLS). A mutant of eIF4E with the N-terminal tail shorter by five amino acids (33-217) was used. It is known that affinities of cap analogues to the full length human eIF4E [25] and the truncated murine eIF4E (28-217) [12] are approximately the same, and the three forms of murine eIF4E, i.e., full length, (28-217) and (33-217), give the same translation efficiency in biological assays [11]. These data suggest that the 32-amino acid long, disordered N-terminal portion of eIF4E is dispensable for cap recognition, and prove that the differences between the eIF4E (28-217) and (33-217) forms should only reflect the properties of the local environment of the N-tail, where binding of the other translation factors, eIF4G and 4E-BPs, takes place [35].

While *apo*-eIF4E (28-217) was monomeric in solution [11], *apo*-eIF4E (33-217) has been found to aggregate (table 2). Only rough estimates of the apparent hydrodynamic radius (R_h) of the eIF4E aggregates could be registered, since the quantitative polydispersity

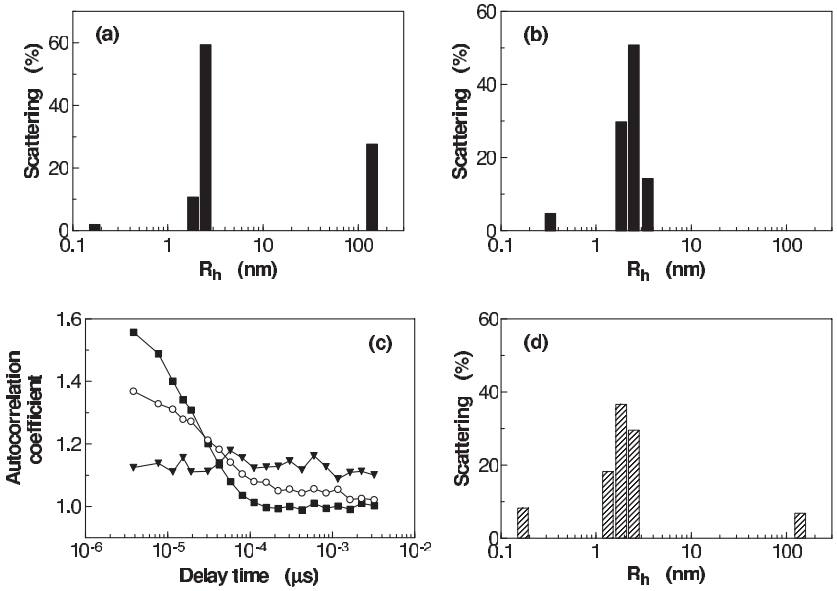

Figure 3. Hydrodynamic studies on eIF4E deaggregation upon interaction with the mRNA 5′ cap. Regularization histograms for dynamic light scattering on a solution containing eIF4E (33-217) and 50-fold excess of m^7GTP (a) after 1 h incubation, (b) after 24 h incubation. (c) Changes of the autocorrelation function in the time of incubation with m^7GTP (▼, before addition of m^7GTP; ○, after 1 h incubation; ■, after 24 h incubation). (d) Regularization histogram for eIF4E (33-217) in the presence of 50-fold excess of $m_3{}^{2,2,7}$GTP after 24 h incubation.

Table 2. Hydrodynamic parameters for eIF4E-cap complexes of different affinity (K_{as} [a]), which have been obtained by means of dynamic light scattering; hydrodynamic radius (R_h), polydispersity index (PDI), diffusion coefficient (D), and multi-modal size distribution (1st, 2nd and 3rd mean of R_h, see figure 3) corresponding to water (∼0.2 nm), monomeric eIF4E-cap complexes (∼2 nm), and to non-specific aggregates (>100 nm).

Protein form	K_{as} [a] $\times 10^{-6}$ (M^{-1})	$R_h \pm \Delta R_h$ (nm)	PDI	D $\times 10^7$ (cm s^{-2})	1st mean R_h (nm)	2nd mean R_h (nm)	3rd mean R_h (nm)
apo-eIF4E		∼40		∼1.12			
$m_3{}^{2,2,7}$GTP + eIF4E	0.143	2.98 ± 1.4	0.55	7.71	0.17	1.99	140
m^7Gpppm^{7}G + eIF4E [b]	1.93	2.30 ± 0.7	0.11	9.31	0.22	2.36	
m^7GpppG + eIF4E	7.39	2.40 ± 0.7	0.095	8.94	0.24	2.41	
m^7Gppppm^{7}G + eIF4E [b]	23.5	2.38 ± 0.7	0.10	8.98	0.17	2.45	
p-Cl-bz^7-GTP + eIF4E	44.6	2.55 ± 0.8	0.12	8.42	0.17	2.28	
m^7GppppG + eIF4E	102.8	2.38 ± 0.65	0.095	8.98	0.17	2.42	
m^7GTP + eIF4E	108.7	2.36 ± 0.7	0.11	9.07	0.33	2.44	

[a] Data from [12].
[b] The microscopic association constant ($K_{as}^{micro} = 0.5K_{as}$) has been taken into account.

index was unmeasurable. Addition of one of the cap analogues, i.e., m^7GTP, *p*-Cl-bz^{7}GTP, $m_3{}^{2,2,7}$GTP, m^7GpppG, m^7Gpppm^{7}G, m^7GppppG, or m^7Gppppm^{7}G, to the aggregated eIF4E samples caused progressive deaggregation (figure 3). After 24 h of incubation of eIF4E with the cap analogues which had association constants of the order of 10^6–10^8 M^{-1} [12], the eIF4E-cap complexes were characterized by average values of MW = 24.1 kDa

and $R_h = 2.39$ nm with standard deviations among the cap analogues of 1.9 kDa and 0.07 nm, respectively. The uncertainty of determination of the R_h values from DLS due to polydispersity of the solution was 0.7 nm. These values measured for the hydrated complexes in solution correspond to the monomeric state of eIF4E, since the crystallographically determined diameters of this approximately globular protein in the complex with m^7GTP are 4.1 nm × 3.6 nm × 4.5 nm [11].

In contrast to the strongly binding cap analogues, $m_3{}^{2,2,7}$GTP did not cause entire deaggregation, and the eIF4E-$m_3{}^{2,2,7}$GTP solution was polydispersed. The DLS data revealed the presence of the eIF4E aggregates which had a hydrodynamic radius of $R_h \sim 140$ nm (table 2, figure 3). This cap analogue is an unspecific ligand of eIF4E and binds with an association constant of only 10^5 M^{-1} [12]. During the control measurements, the *apo*-protein remained still completely aggregated, even when ultrasonication had been applied.

Together, these data show that deaggregation of eIF4E in the presence of the cap analogues occurred under the influence of specific interaction with the mRNA 5′ cap structure.

4. Conclusions

Conformational changes of the initiation translation eIF4E factor upon binding to the mRNA 5′ cap structure have been investigated from the thermodynamic and hydrodynamic point of view by fluorescence spectroscopy and dynamic light scattering, respectively.

The eIF4E-cap interaction is related to favourable enthalpy changes. The entropy changes can be either positive or negative, depending on the chemical alterations introduced into the cap structure. Positive heat capacity changes that accompany the binding suggest significant differences in accessibility of the protein hydrophobic surface to the solvent for the *apo*-eIF4E and for the complex with a cap. eIF4E has been shown to be a highly fluctuating protein unless it is bound to the specific ligands, i.e., the chemical 5′ cap analogues. Then the fluctuations are silenced and the protein in the complex becomes more stiff.

The DLS measurements showed that the protein aggregation–deaggregation equilibrium is influenced by specific interaction with the cap analogues. This indicates that association of eIF4E with the cap results in conformational transitions after which the region of the eIF4E molecular surface engaged in the aggregation is no longer capable of binding the second eIF4E molecule. The proneness to aggregation is highly dependent on the length of the N-terminus, which is close to the eIF4G and 4E-BPs binding site at the hydrophobic dorsal surface of eIF4E. Hence, this surface is likely to be mostly modified upon cap-binding, which is concordant with the data on cooperativity of the two binding sites of eIF4E [12, 38]. On the other hand, these results suggest a possible regulatory role of the evolutionally divergent and spatially disordered N-terminus of eIF4E during protein–protein interactions.

Acknowledgments

We thank Professor Stephen Burley for enabling access to his DLS facility, Dr Janusz Stepinski and Dr Marzena Jankowska-Anyszka for providing the cap analogues, Professor Nahum Sonenberg for the eIF4E plasmids, and Lilia Zhukova for eIF4E expression and purification. This research was supported by the Polish Committee for Scientific Research (KBN 3 P04A 021 25, KBN PBZ 059/T09/10, BST 975/BF) and the Fogarty International Center, NIH (1 R03 TW006446).

References

[1] Muthukrishnan S, Both G W, Furuichi Y and Shatkin A J 1975 *Nature* **255** 33–7
[2] Lewis J D and Izaurralde E 1997 *Eur. J. Biochem.* **247** 461–9

[3] Izaurralde E, Stepinski J, Darzynkiewicz E and Mattaj I W 1992 *J. Cell Biol.* **118** 1287–95
[4] Mattaj I W 1986 *Cell* **46** 905–11
[5] Hamm J, Darzynkiewicz E, Tahara S M and Mattaj I W 1990 *Cell* **62** 569–77
[6] Sharp P A 1994 *Cell* **77** 805–15
[7] Sonenberg N, Morgan M A, Merrick W C and Shatkin A J 1978 *Proc. Natl Acad. Sci. USA* **75** 4843–7
[8] Sonenberg N 1996 *Translational Control* ed J W B Hershey, M B Mathews and N Sonenberg (Cold Spring Harbor, NY: CSHL Press) pp 245–69
[9] Joshi B, Cai A L, Keiper B D, Minich W B, Mendez R, Beach C M, Stepinski J, Stolarski R, Darzynkiewicz E and Rhoads R E 1995 *J. Biol. Chem.* **270** 14597–603
[10] Zuberek J *et al* 2003 *RNA* **9** 52–61
[11] Marcotrigiano J, Gingras A C, Sonenberg N and Burley S K 1997 *Cell* **89** 951–61
[12] Niedzwiecka A *et al* 2002 *J. Mol. Biol.* **319** 615–35
[13] Tomoo K *et al* 2002 *Biochem. J.* **362** 539–44
[14] Blachut-Okrasinska E, Bojarska E, Niedzwiecka A, Chlebicka L, Darzynkiewicz E, Stolarski R, Stepinski J and Antosiewicz J M 2000 *Eur. Biophys. J.* **29** 487–98
[15] Niedzwiecka A, Stepinski J, Darzynkiewicz E, Sonenberg N and Stolarski R 2002 *Biochemistry* **41** 12140–8
[16] Strudwick S and Borden K L 2002 *Differentiation* **70** 10–22
[17] Dostie J, Lejbkowicz F and Sonenberg N 2000 *J. Cell Biol.* **148** 239–47
[18] Tang S J, Reis G, Kang H, Gingras A C, Sonenberg N and Schuman E M 2002 *Proc. Natl Acad. Sci. USA* **99** 467–72
[19] Hershey J W and Miyamoto S 2000 *Translational Control of Gene Expression* ed N Sonenberg, J W Hershey and M B Mathews (Cold Spring Harbor, NY: CSHL Press) pp 637–54
[20] Nathan C A, Liu L, Li B D, Abreo F W, Nandy I and De Benedetti A 1997 *Oncogene* **15** 579–84
[21] Miyamoto S, Kimball S R and Safer B 2000 *Biochim. Biophys. Acta* **1494** 28–42
[22] Zuberek J, Jemielity J, Jablonowska A, Stepinski J, Dadlez M, Stolarski R and Darzynkiewicz E 2004 *Biochemistry* **43** 5370–9
[23] Darzynkiewicz E, Ekiel I, Tahara S M, Seliger L S and Shatkin A J 1985 *Biochemistry* **24** 1701–7
[24] Edery I, Altmann M and Sonenberg N 1988 *Gene* **74** 517–25
[25] Niedzwiecka-Kornas A, Chlebicka L, Stepinski J, Jankowska-Anyszka M, Wieczorek Z, Darzynkiewicz E, Rhoads R E and Stolarski R 1999 *Collect. Symp. Ser.* **2** 214–8
[26] Ha J H, Spolar R S and Record M T Jr 1989 *J. Mol. Biol.* **209** 801–16
[27] Eftink M R, Anusiem A C and Biltonen R L 1983 *Biochemistry* **22** 3884–96
[28] Niedzwiecka A, Darzynkiewicz E and Stolarski R 2004 *Biochemistry* **43** 13305–17
[29] Beyer W H 1987 *CRC Standard Mathematical Tables* (Boca Raton, FL: CRC Press)
[30] Taylor J R 1982 *An Introduction to Error Analysis* (Mill Valley, CA: University Science Books)
[31] Brunner H and Dransfeld K 1983 *Biophysics* ed W Hoppe, W Lohmann, H Markl and H Ziegler (New York: Springer) pp 93–100
[32] Koppel D E 1972 *J. Chem. Phys.* **57** 4814–20
[33] Martz E 2002 *Trends Biochem. Sci.* **27** 107–9
[34] Sturtevant J M 1977 *Proc. Natl Acad. Sci. USA* **74** 2236–40
[35] Marcotrigiano J, Gingras A C, Sonenberg N and Burley S K 1999 *Mol. Cell* **3** 707–16
[36] Krug R R, Hunter W G and Grieger R A 1976 *Nature* **261** 566–7
[37] Sharp K 2001 *Protein Sci.* **10** 661–7
[38] von der Haar T, Ball P D and McCarthy J E 2000 *J. Biol. Chem.* **275** 30551–5
[39] Wieczorek Z, Stepinski J, Jankowska M and Lonnberg H 1995 *J. Photochem. Photobiol.* B **28** 57–63
[40] Dawson R M, Elliott D C, Elliott W H and Jones K M 1969 *Data for Biochemical Research* (Oxford: Clarendon)
[41] Ruszczynska K, Kamienska-Trela K, Wojcik J, Stepinski J, Darzynkiewicz E and Stolarski R 2003 *Biophys. J.* **85** 1450–6